Journal of Solid State Chemistry **150,** 404–409 (2000)
doi:10.1006/jssc.1999.8616, available online at http://www.idealibrary.com on IDEAL®

Crystal Structure of $SrAl_2B_2O_7$ and Eu^{2+} Luminescence

F. Lucas, S. Jaulmes, and M. Quarton[1]

Laboratoire de Cristallochimie du Solide, Université Pierre et Marie Curie-Paris 6, 4 place Jussieu, 75252 Paris Cedex 05, France

and

T. Le Mercier, F. Guillen, and C. Fouassier

Institut de Chimie de la Matière Condensée de Bordeaux, Université Bordeaux 1, 162 Avenue du Dr A. Schweitzer, 33608 Pessac Cedex, France

Received June 23, 1999; in revised form December 1, 1999; accepted December 15, 1999

The crystal structure of strontium dialuminodiborate $SrAl_2B_2O_7$ has been established by single-crystal X-ray diffraction methods. The compound crystallizes in the trigonal system (space group $R\bar{3}c$, $Z = 6$) with cell parameters $a = 4.893(1)$ Å and $c = 47.78(1)$ Å. Aluminium and boron atoms are, respectively, in tetrahedral and triangular oxygen coordination. The assembly of Al_2O_7 units and BO_3 triangles forms double layers between which Sr^{2+} ions are located. The Eu^{2+}-doped crystalline powder exhibits a luminescence band with maximum at 415 nm. Luminescence characteristics are compared to those of other strontium borates.

Key Words: **borates; oxides; crystal structure; Eu^{2+} luminescence; optical materials.**

INTRODUCTION

The emission and absorption spectra of Eu^{2+} ions usually consist of broad bands due to transitions between the $^8S_{7/2}$ ($4f^7$) ground state and the crystal field components of the $4f^6 5d$ excited state configuration. Electronic transitions between the $4f^6 5d$ and $4f^7$ configurations have high probabilities because these are parity allowed. The resultant fast-decaying luminescence presents many applications: blue-emitting materials are employed in fluorescent lamps and more recently in plasma display systems and UV-emitting phosphors are employed in lamps for medical applications and skin tanning.

Radiative transitions occur from the lowest levels derived from the $4f^6 5d$ states. Since the involved $5d$ orbitals are external, the position of these energy levels and consequently the wavelength of the maximum of the emission bands strongly depend on the host crystal. Covalency, the strength of the crystal field, and the Stokes shift must be taken into account for the Eu^{2+} emission.

The investigation of the luminescence of Eu^{2+} in numerous strontium borates during the last two decades has shown that the position of the emission band varies from the UV range to red, depending on the host lattice [1–4]. For most borates the emission has low intensity at 300 K. However, a high efficiency has been reported for the UV emission of SrB_4O_7 : Eu at 368 nm [1]. In most aluminates the emission of Eu^{2+} lies in the visible range. In the framework of a search for blue-emitting materials for display application, we investigated the luminescence of divalent europium ions in the compound $SrAl_2B_2O_7$ with regard to its structural features.

The compound $SrAl_2B_2O_7$ was obtained by crystallization of aluminoborate glasses several years ago [5]. The author found two crystalline forms and indexed their X-ray patterns on the basis of a cubic and a hexagonal unit cell. More recently $SrAl_2B_2O_7$ was proposed as a nonlinear optical material and its crystal structure was described with a noncentrosymmetric space group in the trigonal system, but the corresponding crystallographic data were not published [6]. A comparison of X-ray powder diffraction data highlights the complete correspondence between the reported cubic form [5] and the phase that we obtained by solid state reaction. Nevertheless, our own indexation of the powder diffractogram and the data obtained from a single crystal sample are different: this form actually crystallizes in the trigonal system in agreement with the more recent results [6] but it appears centrosymmetric.

EXPERIMENTAL

Preparation Processes

Single crystals were grown by the flux method using SrB_4O_7 in order to avoid contamination by foreign atoms.

[1] To whom correspondence should be addressed. E-mail: mq@ccr.jussieu.fr. Fax: 33-1 44 27 25 48.

0022-4596/00 $35.00

TABLE 1
Crystal Data and Data Collection

$SrAl_2B_2O_7$, Trigonal $R\bar{3}c$ (n°167)
$a_{hex} = 4.893(1)$ Å, $c_{hex} = 47.78(1)$ Å, $V = 990.4(4)$ Å^3, $Z = 6$
$D_x = 2.753$, $D_m = 2.65(8)$ (measured by pycnometry)
Nonius CAD4 diffractometer, Mo$K\alpha$ radiation ($\lambda = 0.71069$ Å)
Crystal size, $158 \times 151 \times 34$ μm
Cell parameters refined from 25 reflections
$\omega/2\theta$ scan, $h = 0 \to 6$, $k = 0 \to 6$, $l = 0 \to 76$
973 measured reflections, 583 conserved in refinement with $I > 3\sigma(I)$
3 standard reflections measured every hour; intensity decay, 0.02%
Absorption correction, analytical [7]; $T_{min} = 0.357$; $T_{max} = 0.756$
21 refined parameters
Extinction coefficient $g = 0.26(6) \times 10^{-6}$ (type I, Gaussian distribution) [8]
$R = 0.043$, $R_w = 0.048$, $w = 1/\sigma(F)$
$(\Delta/\sigma)_{max} = 0.01$, $\Delta\rho_{max} = 0.9$ e cm^{-3}, $\Delta\rho_{min} = -0.8$ e cm^{-3}

An initial mixture of $SrCO_3$, B_2O_3, and amorphous Al_2O_3 in proportions corresponding to a 30% SrB_4O_7–70% $SrAl_2B_2O_7$ ratio was ground, put in a platinum crucible, and heated up to 1000°C. The sample was slowly cooled (5°C h^{-1}) to 600°C and then quenched to room temperature.

Powder samples of a composition $Sr_{1-x}Eu_xAl_2B_2O_7$ ($0 \le x \le 0.10$) were prepared using Eu_2O_3 (99.99% purity), $Sr(NO_3)_2$, H_3BO_3, and $Al(NO_3)_3 \cdot 9H_2O$ as the starting materials. In order to obtain a homogeneous mixture, stoichiometric amounts of starting compounds were dissolved in nitric acid (analytical purity). The solution was then evaporated to dryness. The mixture was treated at 600°C in air in order to eliminate nitrate groups and then the obtained powder was thoroughly ground and heated at 1000°C under a hydrogen flow for 12 h. The purities of all the samples were checked by X-ray diffraction measurements at room temperature using Cu$K\alpha_1$ radiation ($\lambda = 1.54059$ Å). We assumed the reduction to be complete because no presence of Eu^{3+} was detected in diffuse reflectance and emission spectra.

X-Ray and Optical Measurements

Collection of diffracted intensities was performed at 20°C with a Nonius CAD4 four-circle diffractometer. Main acquisition parameters are summarized in Table 1. Collected intensities were first corrected for the Lorentz and polarization effects. Because of the anisotropic shape of the crystal, absorption corrections had to be computed using an analytical method [7]. The structure was solved by Patterson and heavy atom methods then refined with the ORXFLS program [9].

Excitation and emission spectra were recorded with a SPEX Fluorolog 212 fluorescence spectrometer. Excitation spectra were corrected for the variation of the incident flux, as well as emission spectra for the transmission of the monochromator and the response of the photomultiplier. The incident beam was perpendicular to the surface of the sample and the observation angle was equal to 22°. Reflectance spectra were obtained with the same equipment by simultaneously rotating the monochromators placed before and after the sample in order to prevent the luminescence radiation from reaching the detector.

STRUCTURE DETERMINATION OF $SrAl_2B_2O_7$

A single crystal was selected from the melt to record Weissenberg and precession photographs. The patterns indicated a trigonal symmetry with the $R\bar{3}c$ space group.

An automated vertical Philips goniometer was used to obtain a powder diffraction pattern from single crystals ground in an agate mortar. The diffractogram was indexed on the basis of a hexagonal cell using the automatic indexation program Treor [10]. The unit cell parameter values were in agreement with those obtained by the single crystal study; they were refined using the least-squares method.

The Wilson test [11] and a negative test of second harmonic generation with a YAG : Nd laser ($\lambda = 1.06$ μm) were consistent with the centrosymmetric $R\bar{3}c$ space group hypothesis. The density measured by pycnometry (Table 1) was in agreement with that calculated for $Z = 6$ formula units per unit cell.

The strontium atoms are located at the origin on $\bar{3}$ special position (Wyckoff site 6*b*). Afterward electronic density maps obtained from Fourier series gave coordinates of aluminium (12*c* site), oxygen (6*a* and 36*f*), and boron (12*c*). After secondary extinction corrections [8] and convergence of the refinement with anisotropic thermal displacements for all atoms, the final reliability factors were $R = 0.043$ and $R_w = 0.048$. The atomic coordinates and thermal parameters are listed in Table 2. Main values of interatomic distances and interbond angles are given in Table 3.

TABLE 2
Fractional Atomic Coordinates and Thermal Parameters

Atom	x	y	z	U_{eq} (Å^2) $\times 10^3$
Sr	0	0	0	9.2(2)
Al	0	0	0.21514(3)	7.5(4)
B	0	0	0.1326(1)	10(1)
O(1)	0.3950(7)	0.9719(7)	0.03286(7)	13(1)
O(2)	0	0	1/4	23(2)

U_{ij} (Å^2) $\times 10^3$	U_{11}	U_{22}	U_{33}	U_{12}	U_{13}	U_{23}
Sr	8.6(3)	U_{11}	10.3(3)	$U_{11}/2$	0	0
Al	6.8(4)	U_{11}	8.8(6)	$U_{11}/2$	0	0
B	10(2)	U_{11}	11(2)	$U_{11}/2$	0	0
O(1)	11(2)	8(2)	20(2)	5(1)	−4(1)	−2(1)
O(2)	31(3)	U_{11}	9(3)	$U_{11}/2$	0	0

TABLE 3
Selected Geometric Parameters

Distances (Å)		Angles (°)	
Sr–O(1) × 6	2.547(4)		
Sr–O(1) × 6	3.292(4)		
Al–O(2)	1.666(2)	O(1)–Al–O(2) × 3	115.1(2)
Al–O(1) × 3	1.761(3)	O(1)–Al–O(1) × 3	103.3(2)
B–O(1) × 3	1.369(3)	O(1)–B–O(1) × 3	119.82(5)

STRUCTURE DESCRIPTION

The rhombohedral structure of $SrAl_2B_2O_7$ can be described from $(BO_3)_\infty$ planes perpendicular to the trigonal axis (Fig. 1). Each plane is constituted by independent BO_3 triangles. These planes are linked alternatively by Al–O(2)–Al bridges and Sr atoms. The result is a framework of corner-shared AlO_4 tetrahedra and BO_3 triangles. Their assembly by O(1) common vertices forms six-membered rings (Fig. 2). A ring is linked to another by the O(2) remaining apical oxygen atoms of the AlO_4 tetrahedra to build Al_2O_7 units. The strontium atoms, localized in the cavities generated by the six-membered rings, have 12 neighbor oxygen atoms. Six of them are strongly linked with Sr (Table 3) with a bond strength $v = 0.314$ valence unit, the other six are weakly bonded with $v = 0.042$ valence unit [12]. The resulting polyhedron is well approximated by two interlocked octahedra (Fig. 3), but in Fig. 1 one octahedron only is drawn around each Sr atom in order to clarify the representation.

This centrosymmetric structure is the same as that of $CaAl_2B_2O_7$ which has been very recently published [13]. The arrangement of AlO_4 tetrahedra and BO_3 triangles is rigorously the same in the two compounds, due to the covalent nature of the Al–O and B–O bonds. The AlO_4 tetrahedra are distorted with three equal Al–O(1) distances whereas the fourth Al–O(2) bond along the ternary axis is shorter (Table 3), in agreement with the concept of bond valence [14]. The oxygen environment around the boron atom deviates insignificantly from the D_{3h} ideal punctual symmetry: the value of the O–B–O angle is very close to 120° and the distance B–O (1.369 Å) is that calculated by Shannon [15]. So this structure can be viewed as $[Al_2O(BO_3)_2]^{2-}$ covalent layers linked by ionic interactions via the Sr^{2+} cations (Fig. 1). The strontium atoms are regularly distributed in (001) planes according to a hexagonal arrangement (Fig. 2).

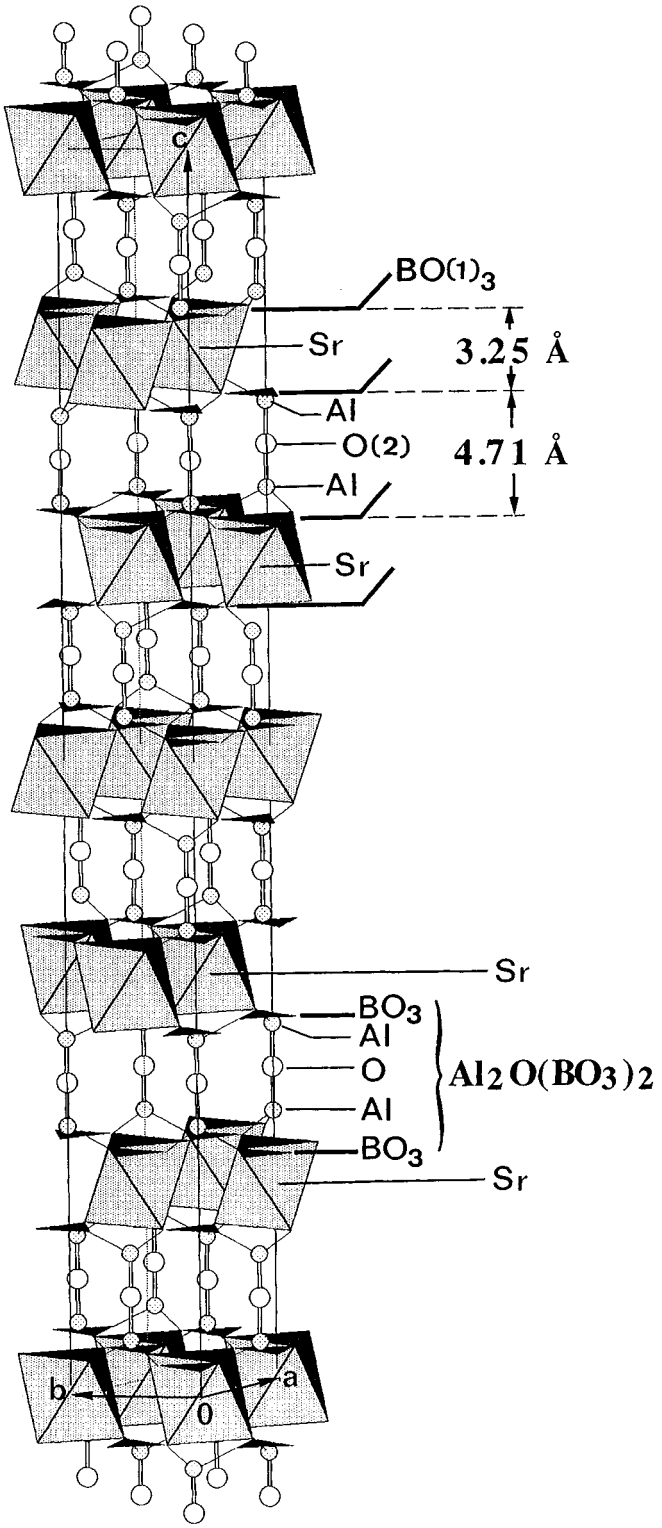

FIG. 1. Perspective view of the structure of $SrAl_2B_2O_7$ with BO_3 triangles and SrO_6 octahedra. Large open circles represent O(2) atoms and small circles represent Al atoms.

LUMINESCENCE OF Eu^{2+} IN $SrAl_2B_2O_7$

At 300 K the maximum of the emission band lies at 415 nm in agreement with what was recently reported by Diaz and Keszler in an investigation of the parameters that govern the position of the Eu^{2+} emission in borates [4]. Figure 4 shows the excitation and emission spectra of $SrAl_2B_2O_7:Eu^{2+}$ (1%) recorded at 9 K. The emission

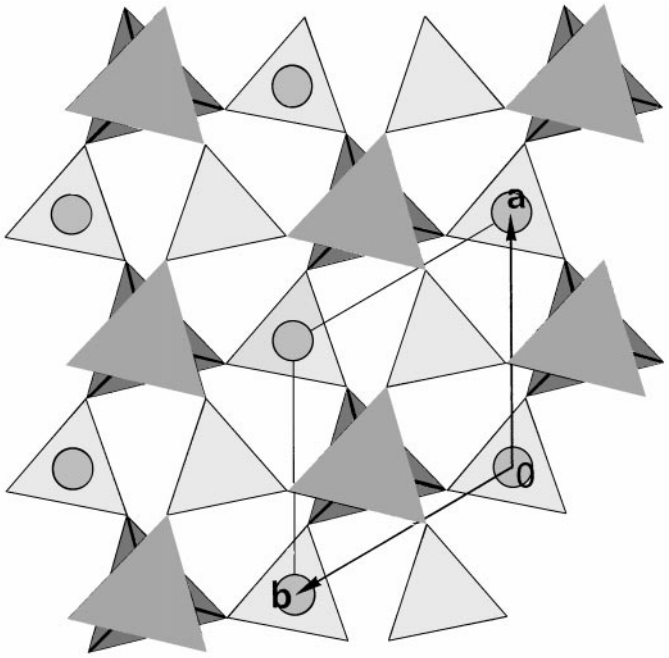

FIG. 2. Projection along trigonal axis of BO_3 triangles (white) and AlO_4 tetrahedra (grey) arrangement. Circles represent Sr atoms.

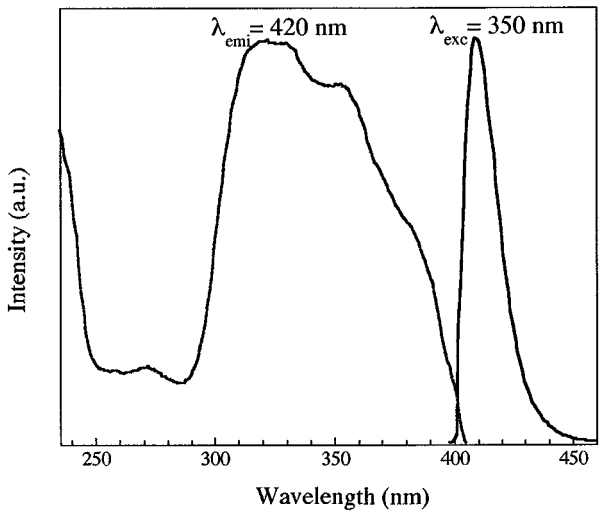

FIG. 4. Excitation and emission spectra of $SrAl_2B_2O_7:Eu^{2+}$ (1%) recorded at 9 K.

spectrum for a 350 nm excitation consists of a band with a maximum of intensity close to 410 nm. The corresponding excitation spectrum presents a structured band between 290 and 405 nm with a maximum around 325 nm and a band below 250 nm. These bands correspond undoubtedly to the divalent europium $4f^7(^8S_{7/2}) \rightarrow 4f^6 5d$ transitions since the unactivated host compound has no absorption in this region. On the basis of the crystal data, one may consider that the divalent europium environment is almost a regular octahedron (the influence of the second neighbors is neglected). The $5d$ orbitals are then expected to split under the crystal field into the E_g and T_{2g} levels. We ascribed therefore the band between 290 and 405 nm to the T_{2g} level, the components of the E_g level being located below 250 nm. The $4f \rightarrow 5d(T_{2g})$ band is split into two components separated by about 2400 cm^{-1} because the real local symmetry is lower than O_h. Moreover, the interaction between the $5d$ electron and the six $4f$ electrons leads to a structure on the low energy side with spacings close to those of the fundamental multiplet ^7F_J ($J = 0$–6) of Eu^{3+} (Fig. 5). Such a structure appears more distinctly in $SrB_4O_7:Eu$ [16] and $M_2B_5O_9X:Eu$ (M = Ca, Sr, Ba; X = Cl, Br) [17]. The Stokes shift calculated from the approximate position of the $4f^6 5d^1$ ($^7F_0$) level in the excitation spectrum amounts to only 700 cm^{-1} at 9 K, a value comparable to that observed by Meijerink and Blasse for $SrB_4O_7:Eu$ (750 cm^{-1}) [16] and $Sr_2B_5O_9Cl:Eu$ (600 cm^{-1}) [17].

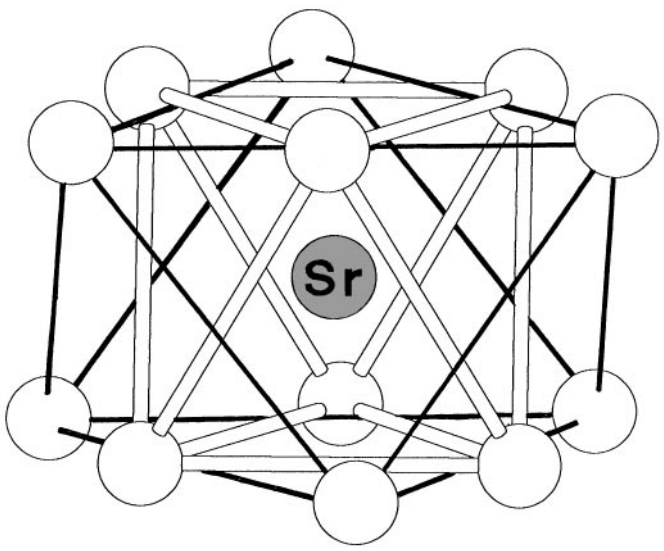

FIG. 3. Strontium oxygen environment constituted by two interlocked octahedra.

More often in the literature the Stokes shift is calculated from the maximum of the lower energy $4f \rightarrow 5d$ transition without taking into account the interactions with $4f$ electrons [4]. In Table 4 the energy of the lower $4f \rightarrow 5d$ transition, the Stokes shift so-calculated, and the emission wavelength at low temperature are compared to those observed in various strontium borates. In B_2O_3-rich hosts, the first excited level lies in the UV range. The covalency of the B–O bond results in a weak nephelauxetic effect and a small ligand field splitting of the $5d$ levels. The stiffness of the host limits the Stokes shift. Consequently, the emission occurs in the UV region. In SrO–rich phases such as $Sr_3(BO_3)_2$ or

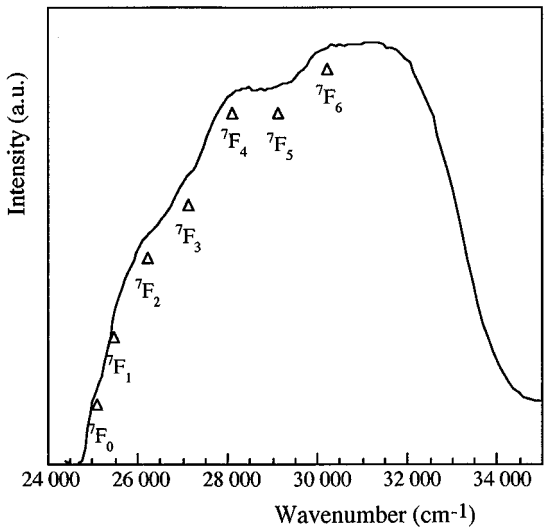

FIG. 5. Splitting of $4f^6$ configuration in lower-energy $4f^65d$ state for $SrAl_2B_2O_7:Eu^{2+}$ (1%) (excitation spectrum at 9 K).

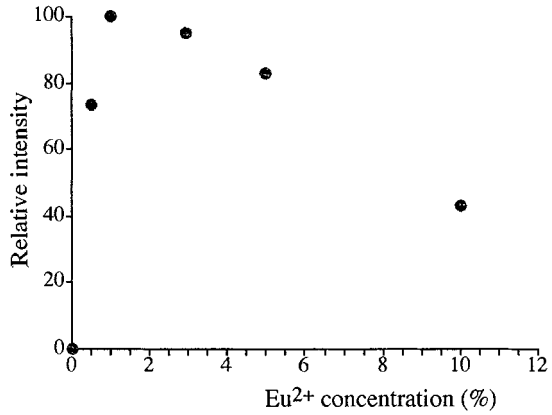

FIG. 6. Europium concentration dependence of emission intensity of $SrAl_2B_2O_7:Eu^{2+}$.

$Sr_2Mg(BO_3)_2$ the energy of the first excited level is considerably lowered. The first $4f \rightarrow 5d$ transitions lie in the visible region. In both structures, oxygen atoms are coordinated by several Sr^{2+} ions [3]. This results in a greater electron density on oxygens. The emission occurs at longer wavelengths in the visible region. As expected because Al–O bonds are less covalent than B–O bonds, the crystal field splitting of the Eu^{2+} $5d$ levels is larger in $SrAl_2B_2O_7$ than in SrB_4O_7, resulting in a shift of the emission to longer wavelengths. The lowering of the emitting state is much less pronounced than in SrO-rich borates. The stabilization of the lower $5d$ level is relatively small since it arises from a small splitting of a triplet state [18].

As shown in Fig. 6, with increasing europium content x, the intensity of the emission band of $SrAl_2B_2O_7:Eu^{2+}$ increases up to $x = 0.01$ and decreases at higher concentrations. Concentration quenching is the result of the migration of the excitation energy among Eu^{2+} ions up to defects.

TABLE 4
Emission Wavelength and Estimated Stokes Shift of Eu^{2+} in Various Strontium Borates

Compound	Lower energy $4f \rightarrow 5d$ transitions (cm^{-1})	Stokes shift (cm^{-1})	λ emission (nm)	Reference
SrB_4O_7	33,100	5900	367	[4, 16]
$SrLiB_9O_{15}$	29,700	4100	390	[4]
$SrAl_2B_2O_7$	28,500	4100	410	This work
$Sr_3(BO_3)_2$	23,300	6000	585	[4]
$Sr_2Mg(BO_3)_2$	22,200	5600	605	[4]

A rough estimate of the critical distance R_c (distance at which the probability of transfer is equal to the probability of radiative emission) can be derived from the concentration x_c above which the quenching of luminescence occurs [19]:

$$R_c \approx 2\left(\frac{3V}{4\pi x_c Z}\right)^{1/3}.$$

R_c is of the order of 30 Å. This high value is the consequence of the small Stokes shift that results in a large overlap of the absorption and emission bands at 300 K. The small Stokes shift is the consequence both of the stiffness of the B–O–Al network and the large size of the site which limits the variation of the Eu–O distance [17].

For $x = 0.01$, absorption of the UV radiation at the maximum of the excitation band is nearly complete. The quantum efficiency is equal to 20% at room temperature. For $SrB_4O_7:Eu$ we obtained an efficiency of 80%.

The temperature dependence of the emission intensity for $x = 0.005$ was examined in the temperature range between 9 and 290 K (Fig. 7). Quenching of the Eu^{2+} emission starts at about 200 K. The temperature at which the intensity has dropped to half of the initial intensity is 260 K. At 290 K only 20% of the intensity remains, in agreement with the measure of the quantum efficiency.

CONCLUSION

In SrB_4O_7 the boron atoms are tetrahedrally coordinated by oxygen atoms. In $SrAl_2B_2O_7$, however, the boron atoms present a triangular oxygen coordination, like in other aluminoborates (e.g., $CaAl_2B_2O_7$ [13], $BaAl_2B_2O_7$ [20], $YAl_3B_4O_{12}$ [21]). The greater ionicity of the Al–O bonds reinforces the covalency of the B–O bonds, favoring a triangular oxygen coordination. The Sr ions are located between double layers composed of AlO_4 tetrahedra and

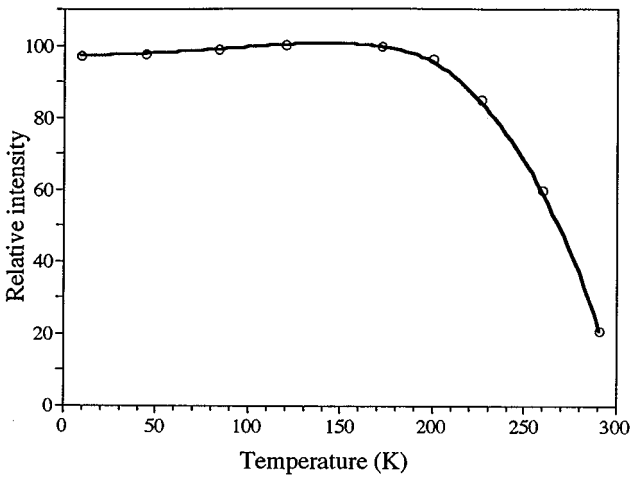

FIG. 7. Temperature dependence of emission intensity between 9 and 290 K of $SrAl_2B_2O_7:Eu^{2+}$ (0.5%).

BO_3 triangles, in large cavities formed by six oxygen atoms at the vertices of an octahedron and six more distant oxygen atoms also with an octahedral arrangement.

The $5d \rightarrow 4f$ emission band of Eu^{2+} is displaced to longer wavelengths with respect to its position in SrB_4O_7. Despite a small Stokes shift, the luminescence efficiency at 300 K is lower than in this borate. The lowering of the emitting level contributes to a decrease in stability. However, the emission of Eu^{2+} in aluminates such as $SrAl_{12}O_{19}$ and $SrAl_2O_4$ with comparable or lower position of the first $4f^6 5d$ state exhibits a much higher stability [22, 23]. The pronounced thermal quenching in $SrAl_2B_2O_7$ is probably caused by the high vibration frequencies of bonds formed by boron in triangular oxygen coordination [24].

ACKNOWLEDGMENTS

This work was supported by Rhodia Recherches. The authors thank Professor D. A. Keszler (Oregon State University, USA) for very pertinent remarks that have improved the quality of this paper.

REFERENCES

1. K. Machida, G. Adachi, and J. Shiokawa, *J. Lumin.* **21,** 101 (1979).
2. W. J. Schipper, D. Van der Voort, P. Van der Berg, Z. A. E. P. Vroon, and G. Blasse, *Mater. Chem. Phys.* **33,** 311 (1993).
3. A. Diaz and D. A. Keszler, *Mater. Res. Bull.* **31,** 147 (1996).
4. A. Diaz and D. A. Keszler, *Chem. Mater.* **9,** 2071 (1997).
5. J. F. MacDowell, *J. Am. Ceram. Soc.* **73,** 2287 (1990).
6. D. A. Keszler, *Curr. Opinion Solid State Mater. Sci.* **1,** 204 (1996).
7. J. De Meulenaer and H. Tompa, *Acta Crystallogr.* **19,** 1014 (1965).
8. P. J. Becker and P. Coppens, *Acta. Crystallogr. Sect. A* **31,** 417 (1975).
9. W. R. Busing, *Acta Crystallogr. Sect. A* **27,** 683 (1971).
10. P. Werner, L. Ericsson, and M. Westdahl, *J. Appl. Crystallogr.* **24,** 987 (1985).
11. A. J. C. Wilson, *Acta Crystallogr.* **2,** 318 (1949).
12. I. D. Brown and D. Altermatt, *Acta Crystallogr. Sect. B* **41,** 244 (1985).
13. K. S. Chang and D. A. Keszler, *Mater. Res. Bull.* **33,** 299 (1998).
14. N. E. Brese and M. O'Keeffe, *Acta Crystallogr. Sect. B* **47,** 192 (1991).
15. R. D. Shannon, *Acta Crystallogr. Sect. A* **32,** 751 (1976).
16. A. Meijerink, J. Nuyten, and G. Blasse, *J. Lumin.* **44,** 19 (1989).
17. A. Meijerink and G. Blasse, *J. Lumin.* **43,** 283 (1989).
18. G. Blasse and A. Bril, *J. Chem. Phys.* **47,** 5139 (1967).
19. G. Blasse, *Philips Res. Rep.* **24,** 131 (1969).
20. C. Chen, N. Ye, B. Wu, W. Zeng, Q. Zhang, C. Zhang, and Y. Zhang, *in* "Proceedings of the International Symposium on Laser and Nonlinear Optical Materials," p. 103, 1997.
21. H. Y. P. Hong and K. Dwight, *Mater. Res. Bull.* **9,** 1661 (1974).
22. A. L. Stevels and A. D. Schrama-de-Pauw, *J. Electrochem. Soc.* **123,** 691 (1976).
23. F. C. Pastilla, A. K. Levine, and M. R. Tomkus, *J. Electrochem. Soc.* **115,** 642 (1968).
24. K. C. Bleijenberg and G. Blasse, *J. Solid State Chem.* **28,** 303 (1979).